



HDAC3 Inhibition Promotes Alternative Activation of Macrophages but Does Not Affect Functional Recovery after Spinal Cord Injury

Selien Sanchez^{1†}, Stefanie Lemmens^{1†}, Paulien Baeten¹, Daniela Sommer¹,
Dearbhaile Dooley², Sven Hendrix^{1‡*} and Myriam Gou Fabregas^{1‡}

¹Department of Morphology, Biomedical Research Institute, Hasselt University, Diepenbeek BE3590, Belgium,

²Health Science Centre, School of Medicine, University College Dublin, Dublin D04 V1W8, Ireland

After spinal cord injury (SCI), monocyte derived macrophages play a detrimental role. Histone deacetylases (HDACs) are central epigenetic regulators of macrophage-polarization. We hypothesized that HDAC3 inhibition suppresses the pro-inflammatory macrophage phenotype (M1), promotes the anti-inflammatory phenotype (M2) and improves functional recovery after SCI. Therefore, two inhibitors of HDAC3 were selected, namely scriptaid and RGFP966. The impact on macrophage polarization was studied by investigating the effect on gene and protein expression of selected M1 and M2 markers. We show that scriptaid differentially influences M1 and M2 markers. It increases CD86 and iNOS gene expression and decreases GPR18, CD38, FPR2 and Arg-1 gene expression as well as the production of IL-6 and NO. RGFP966 primarily increased the expression of the M2 markers Arg-1 and Ym1 and reduced the production of IL-6 (M1). RGFP966 and scriptaid reduced the formation of foamy macrophages. Finally, to investigate the impact of HDAC3 inhibition on functional recovery after SCI, we studied the effects of RGFP966 and scriptaid in an *in vivo* T-cut hemisection SCI model. Histological analyses were performed on spinal cord sections to determine lesion size and astrogliosis, demyelinated area and selected infiltrating immune cells. RGFP966 and scriptaid did not affect functional recovery or histopathological outcome after SCI. In conclusion, these results indicate that specific HDAC3 inhibition with RGFP966 promotes alternative activation of macrophages and reduces the formation of foamy macrophages, but does not lead to a better functional recovery after SCI.

Key words: HDAC3, Spinal cord injury, Macrophages, RGFP966 and Scriptaid

INTRODUCTION

Spinal cord injury (SCI) is a complex disorder, during which, ex-

cessive inflammation and glial scar formation aggravate the tissue damage and have a negative impact on neuronal regeneration [1-7]. Major players in this neuro-inflammatory response are macrophages. These cells react rapidly after injury by producing several cytokines, neurotrophic factors and by playing a role in scar tissue remodelling [8]. Macrophages can be polarized to different subpopulations including *classically activated*- and *alternatively activated macrophages*. This division is an oversimplified yet convenient way to distinguish the many subsets that exist, therefore, throughout this manuscript, these subtypes will be described as

Received July 4, 2018, Revised September 7, 2018,
Accepted September 28, 2018

*To whom correspondence should be addressed.

TEL: 32 11 26 92 46

e-mail: sven.hendrix@uhasselt.be

†Equally contributing first authors.

‡Equally contributing senior authors.

M1 and M2 macrophages, respectively [9, 10]. M1 macrophages exert detrimental effects by attacking dystrophic axons through direct interaction, while M2 macrophages are rather beneficial by reducing the expression of pro-inflammatory cytokines and promoting neurite outgrowth [9, 11-13]. In addition, macrophages become foamy after SCI following phagocytosis of large amounts of spinal cord debris, which in turn, converts them to an M1 phenotype [14]. These specific characteristics along with their plasticity capabilities, make macrophages a promising target after SCI [15].

Histone deacetylases (HDACs) have recently been identified as important therapeutic targets in many human central nervous system (CNS) disorders [16]. HDACs remove acetyl groups from histones or other protein substrates. Protein acetylation modulates the function of many proteins and can therefore affect numerous cellular processes, such as gene transcription, microtubule dynamics, metabolism and aging. Valproic acid (VPA), a broad-acting HDAC inhibitor, has been shown to affect the macrophage phenotype and to improve functional recovery after SCI [17, 18]. Scriptaid, which is a more specific HDAC inhibitor that targets HDAC1, HDAC3 and HDAC8, prevents white matter injury and improves motor functions after traumatic brain injury (TBI). In addition, Wang et al. showed that scriptaid shifted microglia/macrophage polarization towards the protective M2 phenotype [19, 20]. However, the underlying mechanisms and the specific HDAC responsible for these effects, remain unclear. Since, HDAC3 is a key regulator of macrophage polarization, it represents a promising therapeutic target [21].

In this study, we examined the effects of scriptaid and RGFP966, a specific HDAC3 inhibitor, on macrophage polarization and SCI recovery. We hypothesized that HDAC3 inhibition induces the protective macrophage M2 phenotype leading to improved functional recovery after SCI. The influence of both inhibitors on macrophage polarization has been investigated by determining the expression of selected M1 and M2 markers on the gene and protein level. Secondly, the effects of RGFP966 and scriptaid on functional recovery after SCI have been evaluated by assessing the Basso Mouse Scale (BMS) in the T-cut hemisection SCI mouse model. Our results indicate that the specific HDAC3 inhibitor RGFP966 promotes alternative activation of macrophages, but does not lead to better functional recovery after SCI.

MATERIALS AND METHODS

Isolation and differentiation of bone marrow derived macrophages

Bone marrow derived macrophages (BMDMs) were obtained

by isolating primary bone marrow cells from femurs and tibias of female Balb/c mice (Envigo, Cambridgeshire, U.K.) as previously described [22]. These femoral and tibial cell suspensions were flushed out of the bones with sterile ice-cold 1x phosphate-buffered saline (PBS). Cells were cultured and differentiated in RPMI 1640 medium (Lonza, Basel, Switzerland) for 10 days, supplemented with 10% heat-inactivated fetal calf serum (hiFCS; Gibco, Waltham, U.S.A.), 1% penicillin/streptomycin (Sigma-Aldrich, Saint Louis, U.S.A.) and 15% L929 conditioned medium (LCM), at 37°C and 5% CO₂. After 10 days, the differentiated BMDMs were plated out for *in vitro* experiments.

Treatment of BMDMs

For qPCR (1×10^6 cells/condition), western blot (0.5×10^6 cells/condition), the arginase activity assay (1×10^6 cells/condition), the ELISA (0.5×10^6 cells/condition) and the Griess assay (0.5×10^6 cells/condition), the BMDMs were first pre-stimulated for 1 hour either with LPS (200 ng/ml; EMD Millipore, Billerica, U.S.A.) to obtain a polarization towards M1 macrophages or with IL-4 (33 ng/ml; Peprotech, Rocky Hill, U.S.A.) or IL-13 (33 ng/ml; Peprotech) to obtain a polarization towards M2 macrophages (Figs. 1~6). Thereafter, the BMDMs were stimulated for 24 hours with RGFP966 (5 μ M or 10 μ M, Cayman Chemicals, Ann Arbor, U.S.A.) or scriptaid (0.2 μ M or 1 μ M; Sigma-Aldrich). These doses displayed no toxicity. RGFP966 was chosen because it has an IC50 of 0.08 μ M for HDAC3 and showed no effective binding for any other HDAC at concentrations up to 15 μ M [23]. A condition with dimethylsulfoxide (DMSO; Sigma-Aldrich) has been used as a vehicle control. This experimental set-up is shown in Fig. 3A. Pictures were taken of the BMDMs in all these conditions after 24 hours using a Nikon eclipse TS100 microscope, the results are shown in Fig. 2.

For the Oil red O (ORO; 0.75×10^6 cells/condition) assay, BMDMs were stimulated for 1 hour with either LPS or IL-4 to obtain polarization towards an M1 or M2 macrophage phenotype. Next, these macrophages were treated with RGFP966 (5 μ M, 10 μ M) or scriptaid (0.2 μ M, 1 μ M) for 24 hours. After stimulation with the inhibitors, the cells were treated for 48 hours with spinal cord debris (50 μ g), fixated and stained with ORO.

Quantitative polymerase chain reaction

For the quantitative polymerase chain reaction (qPCR) cell lysis was performed with β -mercaptoethanol in RLT-buffer (1:100; RNeasy Mini Kit, Qiagen, Venlo, The Netherlands). mRNA was isolated using RNeasy Mini Kit (Qiagen) following manufacturer's instructions and the mRNA concentration was measured by Nanodrop (Thermo Fisher Scientific, Merelbeke, Belgium). Fur-

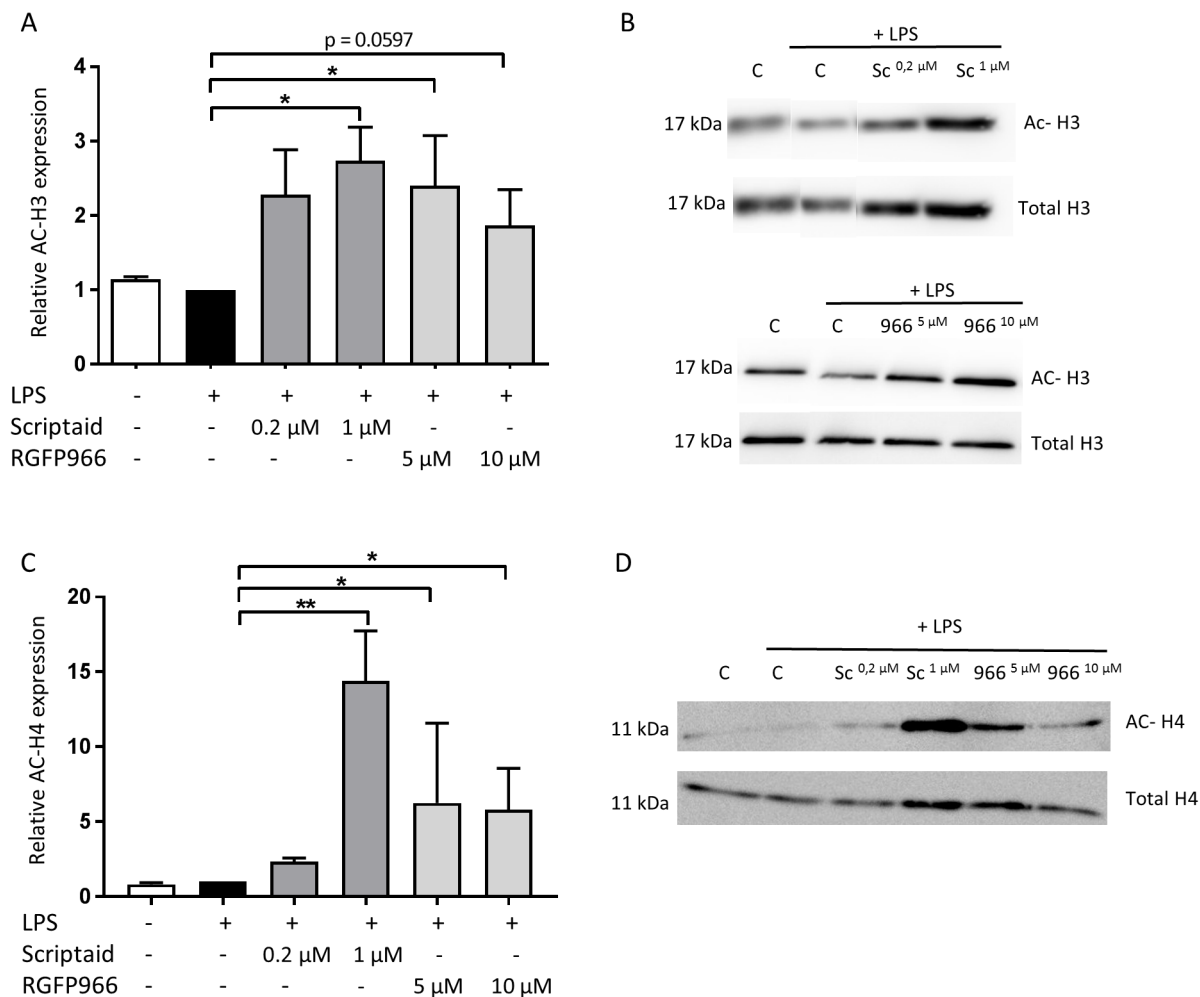


Fig. 1. Scriptaid and RGFP966 increase histone 3 and 4 acetylation. Bone marrow derived macrophages were first stimulated with LPS and after 1 hour these cells were treated with scriptaid or RGFP966 in the indicated concentrations for 24 hours. Total protein lysates were analyzed using western blot to examine if these HDAC inhibitors could potentially increase acetylation of histone 3 and 4. Total Histone 3 and 4 were used as loading control. (A) 1 μ M scriptaid significantly increased histone 3 acetylation at 1 μ M and 5 μ M RGFP966 significantly increased histone 3 acetylation. (C) 1 μ M scriptaid significantly increased histone 4 acetylation and 5~10 μ M RGFP966 significantly increased histone 4 acetylation. (B and D) Representative blots are shown. Data are represented as relative values compared to control+LPS \pm SEM; * p <0.05, ** p <0.01; n =4 biological replicates; AC-H3, acetylation histone 3; AC-H4, acetylation histone 4; LPS, lipopolysaccharide; Sc, scriptaid; C, vehicle control; 966, RGFP966.

thermore, the reverse transcription to cDNA and the qPCR reaction was performed as previously described, the primer sequences that were used are displayed in Table 1 [6]. Relative quantification of gene expression was accomplished with the comparative Ct method. Data were normalized to YWHAZ and HMBS, which were selected as the most stable reference genes using geNorm.

Western blot analysis

Stimulated BMDMs were lysed in SDS lysis buffer (2% (w/v) in 125 mM Tris) to collect total protein lysates. Using Pierce BCA protein assay kit (Thermo Fisher Scientific) according to manufacturer's instructions and iMARK Microplate Reader (Bio-

Rad Laboratories, Hercules, U.S.A.), protein concentrations were measured. Protein samples (10 μ g) were separated on 12% or on 7.5% (for iNOS) SDS gels for 45 minutes at 200 V. The western blot was performed as previously described [6]. The primary antibodies used were: rabbit anti-mouse acetylated histone 3 (1/2000; Cell signalling, Leiden, The Netherlands), goat anti-mouse arginase-1 (Arg-1; 1/1000; Santa Cruz Technologies, Dallas, U.S.A.), mouse anti-mouse inducible nitric oxide synthase (iNOS; 1/500; Sigma-Aldrich), mouse anti-mouse β -actin (1/5000, Santa Cruz). The measured values were normalized to the level of β -actin or total histone 3 and 4, as internal controls. Selected blots (Fig. 1B, 5D and 6B), which derive each from the same membrane have been cut



Fig. 2. Scriptaid and RGFP966 alter macrophage phenotype. Bone marrow derived macrophages were first pre-stimulated with LPS (F), IL-4 (K) or IL-13 (P) or left unstimulated (=control; A). After 1 hour, these cells were treated with scriptaid (0.2 μ M or 1 μ M) or RGFP966 (5 μ M or 10 μ M) for 24 hours. (A~E) Macrophages treated with scriptaid have a similar morphology compared to control. Treatment with RGFP966 resulted in elongated cells, similar to an M2 phenotype morphology especially in the 10 μ M condition. (F~J) M1 macrophage morphology is shown after LPS treatment. Both HDAC3 inhibitors lead to elongated cells, especially after 1 μ M scriptaid and 10 μ M RGFP966 treatment. (K~T) The typical M2 morphology is induced after IL-4 and IL-13 treatment. Scriptaid-treated cells resemble control cells. RGFP966 treatment does not change the M2 morphology as induced by IL-4 and IL-13. Sc, scriptaid; 966, RGFP966; LPS, lipopolysaccharide; IL-4, interleukin-4; IL-13, interleukin-13.

and reordered to increase readability.

Arginase activity assay

Cell pellets from BMDMs stimulated with IL-4 or IL-13 were collected to measure the arginase activity, which is a characteristic of M2 polarisation. The assay was performed using the 'Arginase activity assay kit' (Sigma-Aldrich) according to the manufacturer's instructions.

ELISA IL-6

IL-6 production, which is a characteristic of M1 polarisation, was measured in medium of LPS stimulated cells. The assay was performed using the 'eBioscience Mouse IL-6 ELISA Ready-SET-Go Kit' (Thermo Fisher Scientific) according to the manufacturer's protocol.

Griess assay

To measure nitrite (NO_2^- concentration), which is a measure of NO production and a characteristic of M1 polarisation, a Griess assay was performed on LPS stimulated cell media. This assay was performed using the 'Griess reagent system' kit (Promega, Leiden, The Netherlands) according to the manufacturer's instructions.

Oil red O staining

After culturing and stimulation (Treatment of BMDMs) as previously described, BMDMs were fixed using 4% paraformaldehyde (Sigma-Aldrich) and stained with ORO (Sigma-Aldrich). The staining was extracted using isopropanol and its absorbance was measured at 490 nm using an iMARK Microplate Reader (Bio-Rad Laboratories).

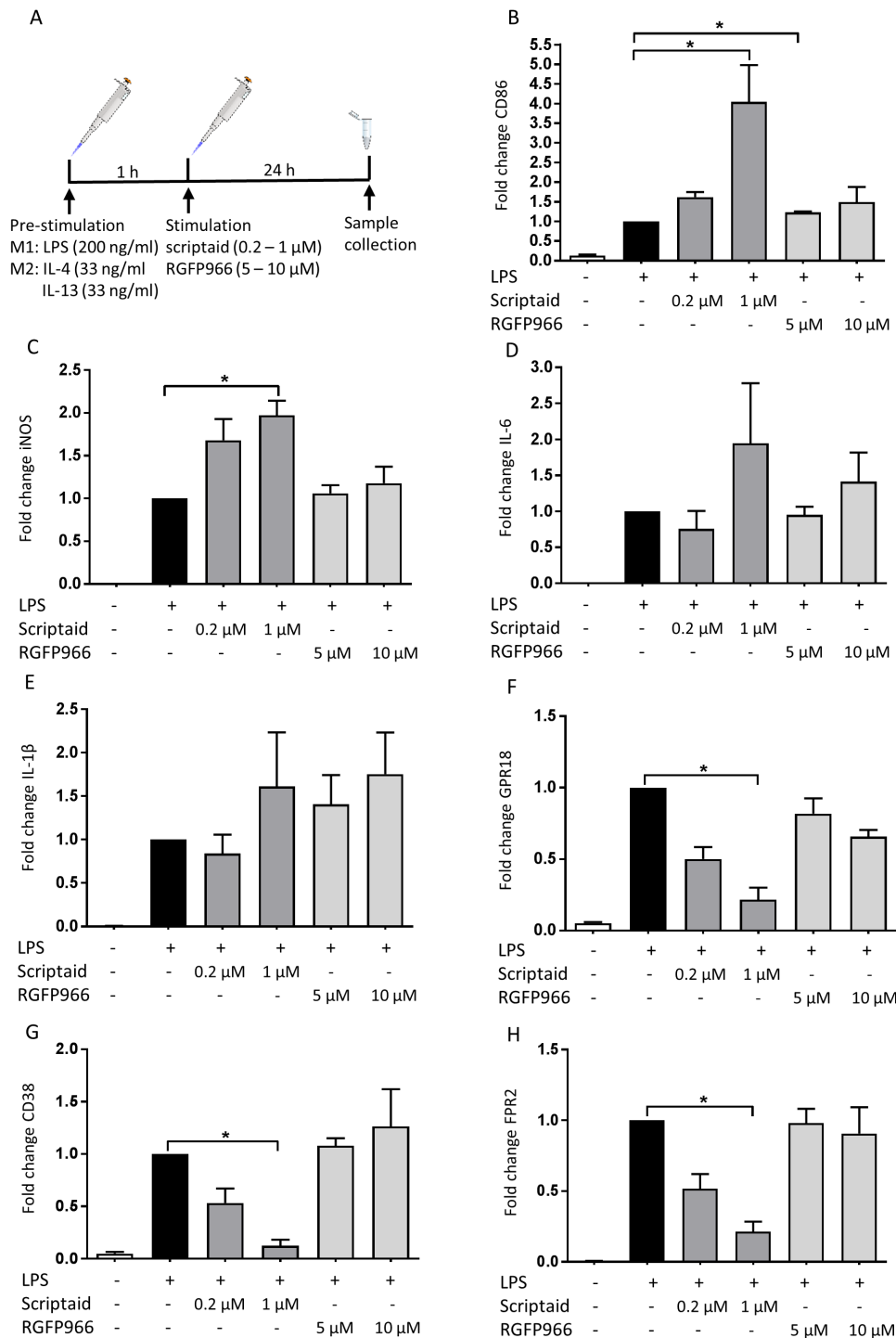


Fig. 3. Scriptaid increases CD86 and iNOS and decreases GPR18, CD38 and FPR2 gene expression, whereas RGFP966 only increases CD86 gene expression. (A) Experimental set-up of the *in vitro* experiments: BMDMs were first pre-stimulated for 1 hour either with LPS (200 ng/ml; M1 macrophages) or with IL-4 (33 ng/ml) or IL-13 (33 ng/ml; M2 macrophages). Thereafter, the BMDMs were stimulated for 24 hours with scriptaid (0.2 μM and 1 μM) or RGFP966 (5 μM and 10 μM). (B–H) M1 macrophages treated with scriptaid or RGFP966 were lysed and RNA was collected for gene expression analysis of several M1 genes: CD86 (B), iNOS (C), IL-6 (D), IL-1β (E), GPR18 (F), CD38 (G) and FPR2 (H). CD86 and iNOS were increased after treatment with 10 μM scriptaid. However, GPR18, CD38 and FPR2 were decreased after treatment with 10 μM scriptaid. CD86 showed a slight increase in gene expression after treatment with 5 μM RGFP966, all other genes showed no significant difference after treatment with RGFP966. Data is shown as fold-change relative to 'control+LPS'±SEM; *p<0.05; n=3 biological replicates. BMDMs, Bone marrow derived macrophages; LPS, lipopolysaccharide; IL-4, interleukin-4; IL-13, interleukin-13; CD38, cluster of differentiation 38; CD86, cluster of differentiation 86; FPR2, formyl peptide receptor 2; GPR 18, G protein-coupled receptor 18; IL-6, interleukin 6; iNOS, inducible nitric oxide synthase.

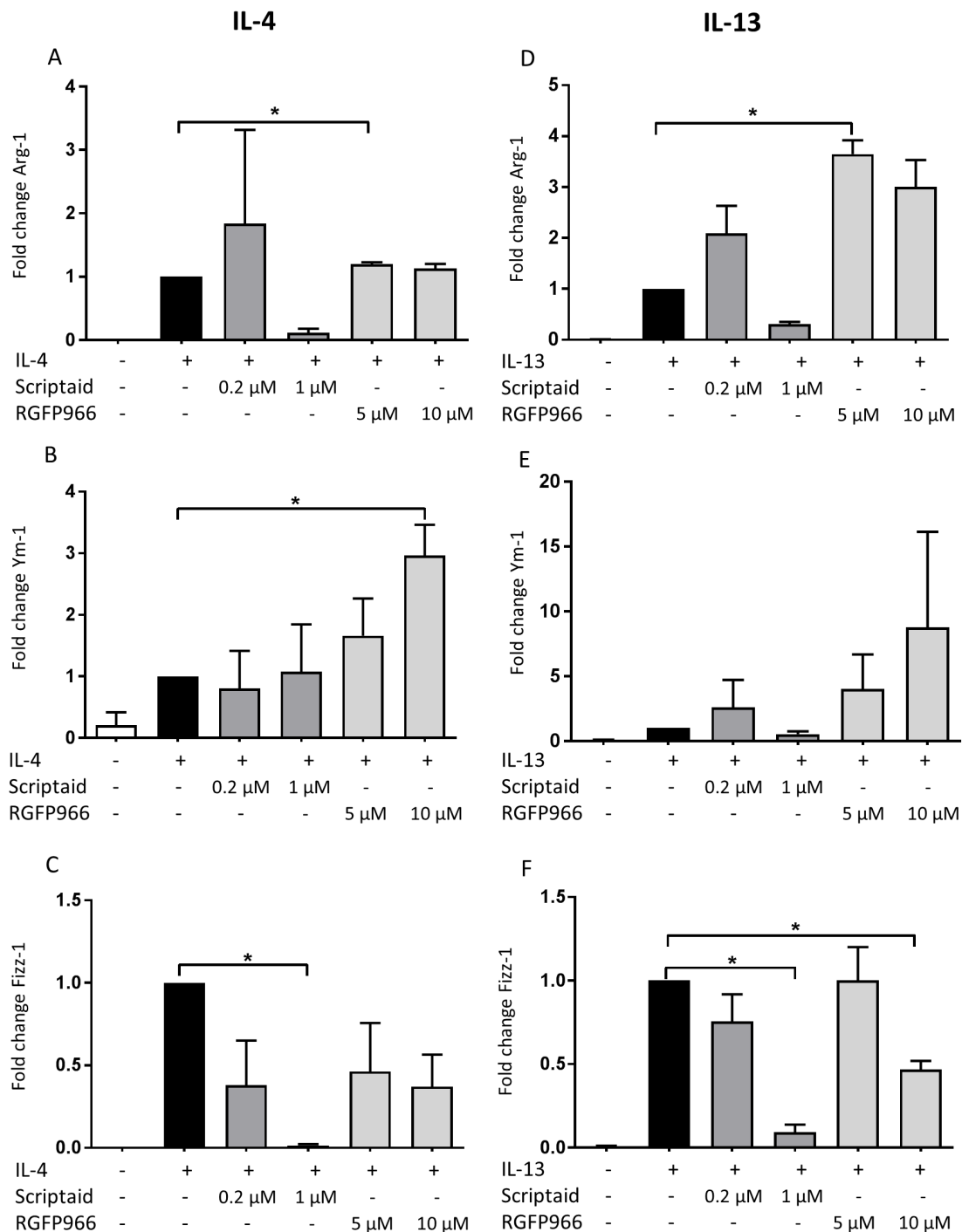


Fig. 4. Scriptaid decreases Fizz-1 gene expression, whereas RGFP966 increases Arg-1 and Ym-1 gene expression and decreases Fizz-1 gene expression. BMDMs were first stimulated with either IL-4 or IL-13 for 1 hour and afterwards treated with scriptaid at 0.2 μ M and 1 μ M or with RGFP966 at 5 μ M and 10 μ M for 24 hours. Next, the cells were lysed and RNA was collected for gene expression analysis of several M2 genes: Arg-1 (A, D), Ym-1 (B, E) and Fizz1 (C, F). (A~C) When stimulated with IL-4, there was no effect of scriptaid on gene expression of Arg-1 or Ym-1. However, there was a decrease in gene expression of Fizz-1 upon scriptaid treatment. Stimulation with IL-4 increased the gene expression of Arg-1 and Ym-1 when treated with RGFP966, there was no effect on gene expression of Fizz-1. (D~F) When stimulated with IL-13, there was no effect on gene expression of Arg-1 or Ym-1 when treated with scriptaid. Gene expression of Fizz-1 was decreased when treated with scriptaid. Stimulation with IL-4 increased the gene expression of Arg-1 and Ym1 when treated with RGFP966, there was no effect on gene expression of Fizz-1. Data is shown as fold-change relative to 'control+IL-4' (A~C) or 'control+IL-13' (D~F) \pm SEM; * p <0.05; n =3 biological replicates. BMDMs, Bone marrow derived macrophages; IL-4, interleukin-4; IL-13, interleukin-13; Arg-1, arginase-1; Fizz-1, found in inflammatory zone; Ym-1, chitinase-like 3.

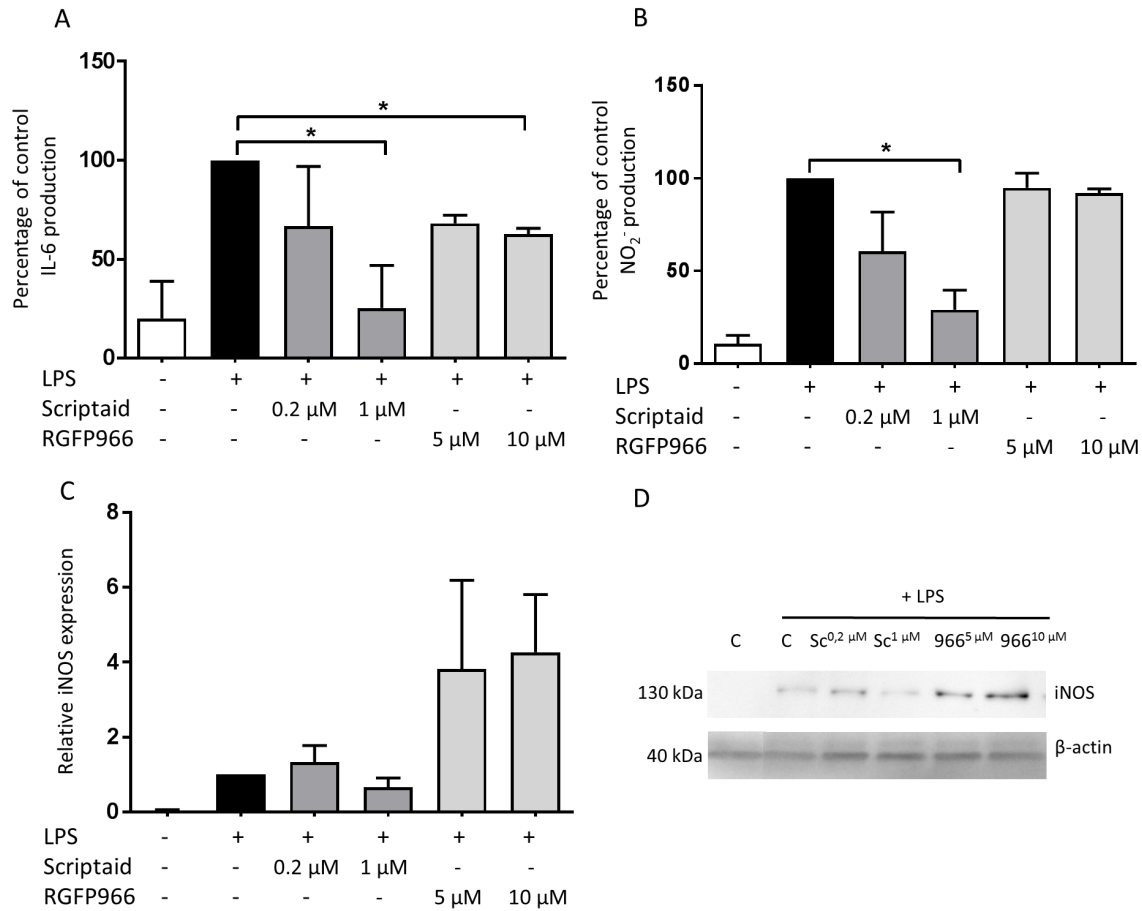


Fig. 5. Scriptaid reduces IL-6 and NO production and RGFP966 reduces IL-6 production. BMDMs were first stimulated with LPS for 1 hour and treated with scriptaid at 0.2 μ M and 1 μ M or with RGFP966 at 5 μ M and 10 μ M for 24 hours (A) Culture medium was collected to analyze the IL-6 production via ELISA. Scriptaid and RGFP966 significantly reduce IL-6 production upon LPS stimulation. (B) Culture medium was collected to analyze the NO₂⁻ production via ELISA. Scriptaid significantly reduced NO₂⁻ production upon LPS stimulation. RGFP966 has no effect on the nitrite production upon LPS stimulation. (C, D) Total protein lysates were analyzed using western blot analysis to examine the iNOS protein expression. Scriptaid and RGFP966 had no effect on iNOS production upon LPS stimulation. A representative blot is shown in (D). Data are represented as relative values compared to control+LPS \pm SEM; *p<0.05; n=3-5 biological replicates; BMDMs, Bone marrow derived macrophages; LPS, lipopolysaccharide; IL-6, interleukin 6; NO₂⁻, nitrite; iNOS, nitric oxide synthase; Sc, scriptaid; C, vehicle control; 966, RGFP966.

Experimental spinal cord injury and HDAC inhibitor treatment

Experiments were performed using 10-week old female Balb/c mice (Envigo). The animals were housed in groups under regular conditions (temperature- and humidity-controlled, 12-hour light/dark cycle and food and water *ad libitum*) in a conventional animal facility at Hasselt University. All experiments were performed according to international standards described in European Communities Council directive 2010/63 and were approved by the local ethical committee of Hasselt University.

T-cut spinal cord hemisection injury was performed as previously described [4-7, 24]. Mice were anesthetized with 3% isoflurane (Isoflo, Abbot Animal Health, Waver, Belgium) and received a subcutaneous injection of the analgesic buprenorphine Temgesic (0.1 mg/kg bodyweight; Val d'Hony Verdifarm, Beringen, Bel-

gium). A partial laminectomy was performed at thoracic level T8 to expose the spinal cord. Iridectomy scissors were used to transect left and right dorsal funiculus, the dorsal horns and the ventral funiculus. This "T-cut" procedure results in a specific and clean transection of the dorsomedial and ventral corticospinal tract. The muscles were sutured and the back skin was closed with wound clips (Autoclip, Clay-Adams Co., Inc. Franklin Lakes, US). Glucose solution (20%) was administered intraperitoneally (i.p.) post-op to compensate for any blood loss during surgery. Bladders were manually emptied daily until autonomic control was restored. Mice were treated i.p. for 3 consecutive days, starting 2 hours after SCI with either RGFP966 (10 mg/kg, dissolved in 7.7% DMSO in NaCl), scriptaid (3.5 mg/kg, dissolved in 0.9% DMSO in NaCl) or vehicle containing 0.9% DMSO in NaCl. The treatment protocol

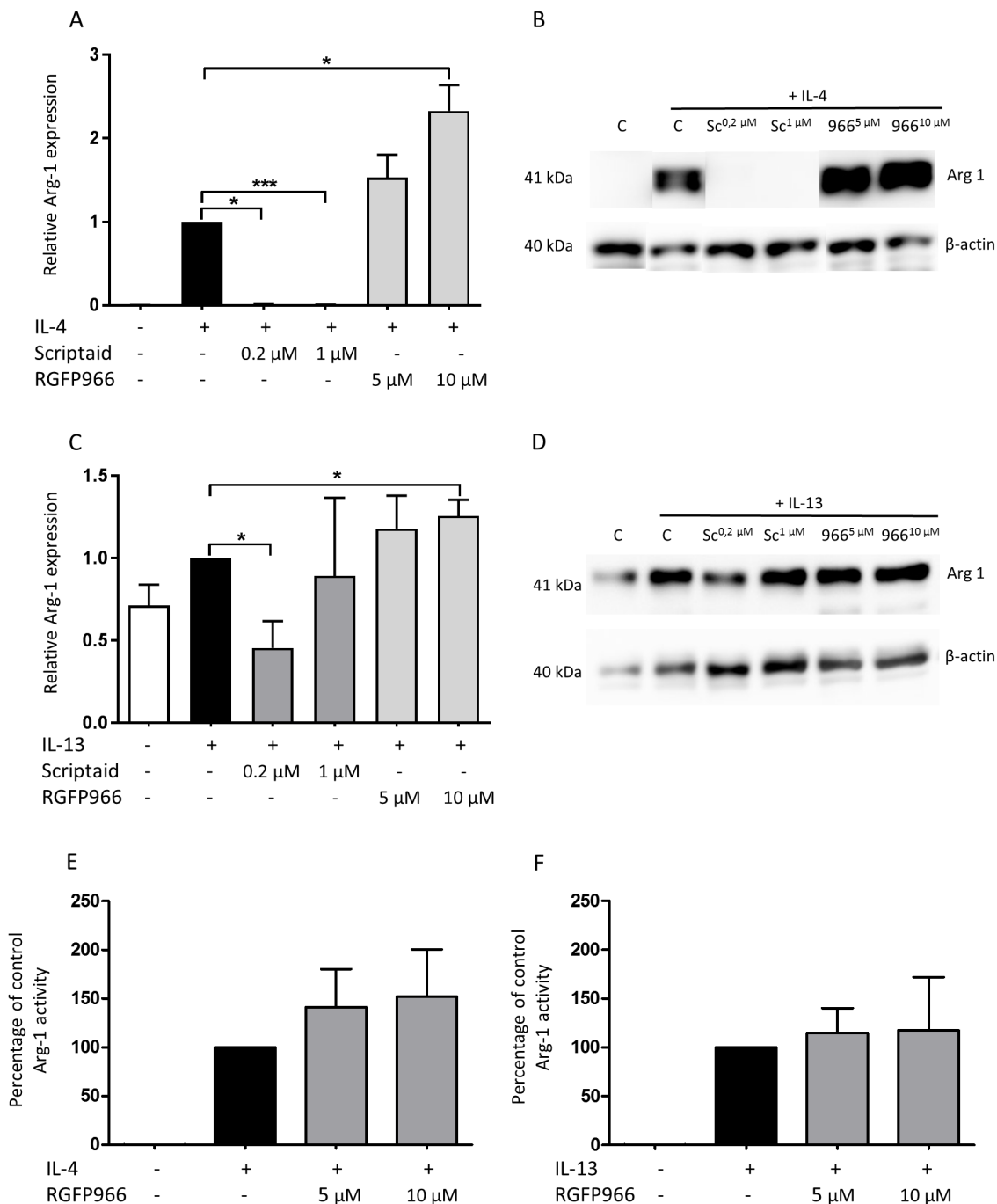


Fig. 6. Scriptaid downregulates Arg-1 expression whereas RGFP966 increases Arg-1 expression. BMDMs were stimulated with IL-4 (A, E) or IL-13 (C, F). After 1 hour, these cells were treated with scriptaid at 0.2 μ M or 1 μ M or with RGFP966 at 5 μ M or 10 μ M for 24 hours. (A~D) Scriptaid significantly downregulated Arg-1 expression upon IL-4 or IL-13 expression. RGFP966 significantly increased Arg-1 expression upon IL-4 and IL-13 stimulation. Representative blots are displayed (B, D). (E, F) RGFP966 had no effect on arginase activity upon IL-4 or IL-13 stimulation. Data represented as percentages relative to 'control+IL-4' (A, E) or 'control+IL-13' (B, F) \pm SEM; n=3 biological replicates; BMDMs, Bone marrow derived macrophages; IL-4, interleukin 4; IL-13, interleukin 13; Arg-1, arginase-1; Sc, scriptaid; C, vehicle control; 966, RGFP966.

was adapted from [25].

Functional recovery in mice was measured using the BMS starting one day after injury until day 27 by a trained investigator

blinded to the experimental groups [26]. In the first week, mice were scored daily and thereafter every other day until the end of the observation period, 27 days post injury (dpi).

Table 1. Primer sequences

Gene	Forward primer	Reverse primer
Arg1	GTGAAGAACCCACGGTCTGT	GCCAGAGATGCTTCCAACCTG
CD38	ACTGGAGAGCCTACCACGAA	TGGGCCAGGTGTTTGGATT
CD86	GAGCGGGATAGTAACGCTGA	GGCTCTCACTGCCTTCACTC
FIZZ1	TCCAGCTAACTATCCCTCCACTGT	GGCCCATCTGTTTCATAGTCTTGA
FPR2	TCTACCATCTCCAGAGTTCTGTGG	TTACATCTACCACAATGTGAACTA
GPR18	CAGACAGGAGGTTCTACATACCA	AGCGAGGCTTGGGTAACAACA
HMBS	GATGGGCAACTGTACCTGACTG	CTGGGCTCCTCTTGGAAATG
IL-1 β	ACCCTGCAGCTGGAGAGTGT	TTGACTTCTATCTTGTGAAGACAAACC
IL-6	TACCACTTCACAAGTCGGAGGC	CTGCAAGTGCATCATCGTTGTTC
iNOS	CCCTTCAATGGTTGGTACATGG	ACATTGATCTCCGTGACAGCC
Ym1	GGGCATACCTTTATCCTGAG	CCACTGAAGTCATCCATGTC
YWHAZ	GCAACGATGTACTGTCTCTTTTGG	GTCCACAATTCCTTCTTGTTCATC

Arg-1, arginase-1; CD38, cluster of differentiation 38; CD86, cluster of differentiation 86; Fizz, found in inflammatory zone; FPR2, formyl peptide receptor 2; GPR 18, G protein-coupled receptor 18; HMBS, hydroxymethylbilane synthase; IL-6, interleukin 6; iNOS, inducible nitric oxide synthase; Ym1, chitinase-like 3; YWHAZ, 14-3-3 protein zeta/delta.

Immunohistochemistry and quantitative image analysis

At 28 dpi, animals were overdosed with dolethal (Vetiquinol NV, Aartselaar, Belgium) and transcardially perfused with ringer-heparin and 4% paraformaldehyde in 0.1 M PBS. Immunofluorescence analysis was performed as previously described [4, 6]. To determine lesion size demyelination, gliosis and inflammatory infiltrate, cryosections were blocked using 10% protein block (Dako Agilent Technologies, Diegem, Belgium) in PBS for 30 minutes at room temperature. Next, the following primary antibodies were incubated overnight at 4°C: mouse anti-GFAP (1/500, Sigma-Aldrich), rat anti-MBP (1/250, EMD Millipore), rabbit anti-Iba-1 (1/350, Wako Chemicals GmbH, Neuss, Germany), rat anti-CD4 (1/25, BD Biosciences, San Jose, U.S.A.). To identify classically or alternatively activated macrophages, sections were permeabilized using 0.1% Triton X-100 for 30 minutes and blocked with 20% donkey serum or 10% goat serum in Tris-buffered saline (TBS, pH 7.5) for 1 hour. Incubation with rat anti-MHC-II (1/200, Santa Cruz Technologies) and goat anti-Arg1 (1/50, Santa Cruz Technologies) primary antibodies was performed overnight at 4 °C. Next, the cryosections were incubated for 1 hour at room temperature with the corresponding secondary antibodies: goat anti-rat IgG Alexa Fluor 568 and 488 (1/250, Invitrogen), goat anti-mouse Alexa Fluor 568 (1/250, Invitrogen), goat anti-rabbit Alexa Fluor 488 (1/250, Invitrogen), donkey anti-goat IgG Alexa Fluor 555 and 488 (1/400, Invitrogen, Carlsbad, U.S.A.), rabbit anti-rat biotin (1/400, Dako) and streptavidin 488 (1/2000, Invitrogen). DAPI (1/1000, Sigma-Aldrich) counterstaining was performed for 10 minutes. Omission of the primary antibody was used to confirm the specificity of the secondary antibodies. All slides were mounted with fluorescent mounting medium (Dako). Fluorescent images were taken using a Leica DM4000 BLED fluorescence microscope with a Leica

DFC450C (Leica microsystems, Diegem, Belgium). Quantitative image analysis was performed using unmodified pictures in ImageJ open source software. GFAP staining was used to evaluate the lesion size by delineating the GFAP- area, in the same way the MBP area was delineated to evaluate the demyelinated area. GFAP and Iba-1 expression was quantified by intensity analysis within rectangular areas of 100 μm \times 100 μm extending 600 μm cranial to 600 μm caudal from the lesion epicentre. CD4⁺ cells were counted in total spinal cord sections, Arg-1⁺ cells and MHCII⁺ cells were counted at the lesion area. The analyses were done on 4~7 spinal cord sections per mouse representing the lesion area, as previously described [4].

Statistical analysis

The analyses were performed using GraphPad Prism 5.0 (GraphPad Software, La Jolla, U.S.A.). D'Agostino and Pearson omnibus normality tests were used to test normal distribution. To compare two groups, a non-parametric Mann-Whitney test was used. When comparing multiple groups, a Kruskal-Wallis with Dunn's multiple comparison was used if normality was not achieved. For functional recovery *in vivo* and histological analyses, a two-way ANOVA for repeated measurements with Bonferroni's post hoc test for multiple comparisons were used. Data were reported as mean \pm standard error of the mean (SEM) and differences were considered significant at $p < 0.05$.

RESULTS

Scriptaid and RGFP966 are potent HDAC inhibitors that induce histone acetylation in macrophages

First, the potency of the HDAC inhibitors scriptaid and

RGFP966 has been confirmed by testing their effects on histone acetylation. The expression of histone 3 and 4 acetylation was analyzed by means of a western blot on total protein lysates from BM-DMs treated with these inhibitors. Both RGFP966 and scriptaid significantly increased histone 3 and 4 acetylation (Fig. 1).

Scriptaid has differential effects on the macrophage phenotype, while RGFP966 promotes the M2 phenotype

Secondly, the effects of scriptaid and RGFP966 were examined on macrophage morphology. Macrophages were left either unstimulated (control) or were stimulated with LPS, IL-4 or IL-13 to obtain M1 or M2 macrophages respectively. As expected, there are clear morphological differences between M0, M1 and M2 macrophages (Fig. 2A~T). M1 macrophages display a flattened, rounded shape while M2 macrophages are more elongated and spindle shaped [27]. Macrophages treated with scriptaid (0.2 and 1 μ M) have a similar morphology compared to control (Fig. 2A~C). Treatment with RGFP966 results in elongated cells, similar to an M2 phenotype morphology especially in the 10 μ M condition (Fig. 2A, D, E). M1 macrophage morphology after LPS treatment is shown in Fig. 2F. Treatment of LPS-pre-stimulated macrophages with both HDAC3 inhibitors leads to elongated cells (Fig. 2G~J), which is most prominent in the higher concentrations (1 μ M scriptaid and 10 μ M RGFP966, Fig. 2H and 2J). In Fig. 2K and 2P the typical M2 morphology is shown after IL-4 and IL-13 treatment respectively. Treatment of these cells with scriptaid make them resemble the control cells (Fig. 2L~M, and Q~R vs. Fig. 2A). Treatment with RGFP966 of the IL-4 and IL-13 pre-stimulated cells does not change the morphology (Fig. 2N~O and S~T vs. Fig. 2K and P).

In a next step, the influence of scriptaid and RGFP966 on the gene expression of selected M1 (CD86, iNOS, IL-6, IL-1 β GPR18, CD38 and FPR2) and M2 (Arg-1, Ym1 and Fizz1) markers was examined. When M1 macrophages were treated with scriptaid, the gene expression of CD86 and iNOS was increased (Fig. 3B, C), while the gene expression levels of GPR18, CD38 and FPR2 were decreased (Fig. 3F~H). There was no effect on the gene expression of IL-6 and IL-1 β (Fig. 3D, E). When M2 macrophages were treated with scriptaid, the gene expression levels of Arg-1 and Ym-1 were not affected (Fig. 4A, B) while Fizz-1 expression was reduced (Fig. 4C). Treating M1 macrophages with RGFP966 had no effect on the gene expression of iNOS, IL-6, IL-1 β , GPR18, CD38 and FPR2 (Fig. 3B~G), but increased the gene expression of CD86 (<0.5-fold change vs control+LPS; Fig. 3B). IL-4-stimulated M2 macrophages showed an increased expression of Arg-1 and of Ym-1 after RGFP966 treatment (Fig. 4A, B). The gene expression level of Fizz-1 was unchanged (Fig. 4C). When the macrophages were treated

with IL-13, there was an increase in Arg-1 gene expression and a decrease in Fizz-1 gene expression after RGFP966 treatment (Fig. 4D~F). There was no effect on the gene expression of Ym-1 (Fig. 4E). Briefly, RGFP966 promoted the gene expression of selected M2 markers (Arg-1 and Ym-1) after IL-4 or IL-13 stimulation and did not affect the expression of the investigated M1 markers (iNOS, IL-6, IL-1 β , GPR18, CD38, FPR2), except for CD86.

Additionally, we investigated the effect of scriptaid and RGFP966 on the protein expression of the M1 markers iNOS, NO and IL-6 [28]. Macrophages were stimulated with LPS to obtain an M1 phenotype followed by treatment with the inhibitors. Both, IL-6 and NO production were significantly downregulated after scriptaid treatment (Fig. 5A, B), while iNOS expression was left unchanged (Fig. 5C). On the protein level, RGFP966 significantly reduced the levels of IL-6 but had no effect on NO production (Fig. 5A, B) and iNOS expression (Fig. 5C).

To further investigate the effects of scriptaid and RGFP966 on macrophage polarization on the protein level, we studied the impact of HDAC3i treatment on the expression of Arg-1, a well-established M2 marker [28, 29]. The macrophages were skewed towards an M2 phenotype using IL-4 or IL-13 followed by scriptaid or RGFP966 treatment. IL-4-induced Arg-1 upregulation is fully eliminated by scriptaid, while IL-13-induced Arg-1 upregulation was only partially reduced (Fig. 6A~D). RGFP966 significantly increased the Arg-1 expression by M2 macrophages (Fig. 6A~D) and had no effect on arginase activity (Fig. 6E, F).

After SCI, foamy macrophages are persistent and become pro-inflammatory due to lipid overload [14]. Since HDAC3 deficiency in macrophages improves their lipid handling [30], we investigated the effects of HDAC3 inhibition on the formation of foamy macrophages. M0, M1 and M2 macrophages were treated with scriptaid and RGFP966 after which they were incubated with spinal cord debris to become foamy, as visualized by ORO staining. Scriptaid did not affect the foaminess of the M0 or M2 macrophages (Fig. 7A, B) but reduced the foaminess of M1 macrophages (Fig. 7C). Analysis of ORO staining's showed that RGFP966 significantly reduced the formation of foamy macrophages regardless of the macrophage phenotype (Fig. 7A~C).

Scriptaid and RGFP966 do not affect functional recovery after SCI

Finally, we investigated the effects of RGFP966 and scriptaid on functional recovery after SCI using the BMS and examined whether HDAC3 inhibition affected lesion size, demyelinated area and immune cell infiltration after SCI. Functional and histological analyses after SCI showed no significant differences between the mice treated with scriptaid and the vehicle control group (Figs.

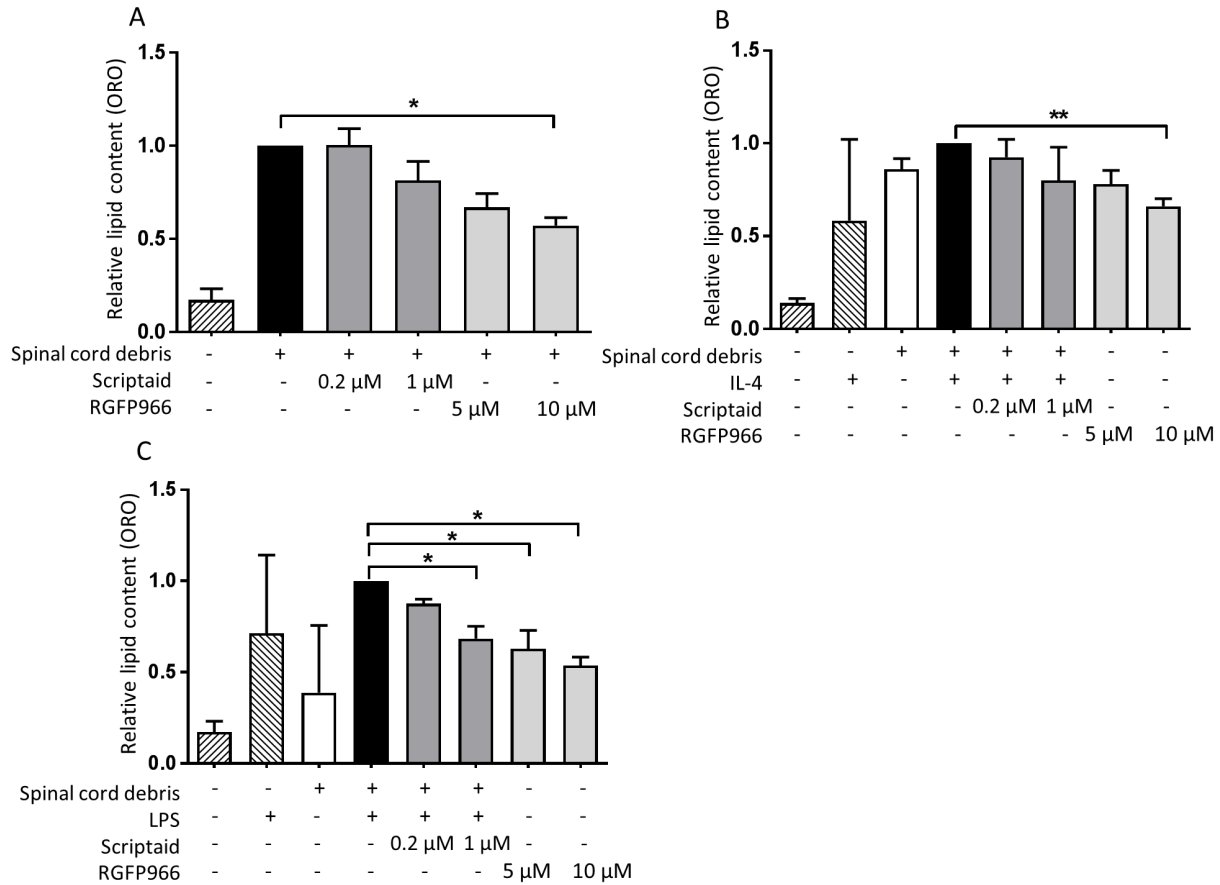


Fig. 7. Scriptaid reduces the formation of foamy macrophages of the M1 phenotype, whereas RGFP966 reduces the formation of foamy macrophages regardless of the phenotype. BMDMs were either left unstimulated (A) or stimulated with IL-4 (B) or LPS (C), after 1 hour these cells were treated with 0.2 μM and 1 μM scriptaid or with 5 μM or 10 μM RGFP966 for 24 hours. Next, cells were treated with spinal cord debris for two days followed by an Oil Red O staining. (A+B) Scriptaid had no effect on the formation of foamy macrophages in unstimulated macrophages or upon IL-4 stimulation. (C) Scriptaid significantly reduced the formation of foamy macrophages of the M1 phenotype. (A~C) RGFP966 significantly reduced the formation of foamy unstimulated macrophages and upon IL-4 and LPS stimulation. Data are shown as relative intensity of absorbance of the Oil Red O staining compared to 'control+spinal cord debris' (A) 'control+IL-4+spinal cord debris' (B) or 'control+LPS+spinal cord debris' (C) (n=3~4 biological replicates; *p<0.05, **p<0.01). BMDMs, Bone marrow derived macrophages; IL-4, interleukin-4; LPS, lipopolysaccharide; ORO, Oil red O.

8~10), except for the level of astrogliosis which were significantly increased in the treatment group compared to the control group (Fig. 8B). Assessing the BMS for 27 days after applying RGFP966 showed no significant difference in functional recovery between the treatment group and the vehicle group (Fig. 8A). On the histological level, there were no differences in lesion size, astrogliosis, demyelinated area and in the numbers of Iba-1, CD4⁺, MHCII⁺ and Arg-1⁺ infiltrating cells between the vehicle group and the group treated with RGFP966 (Figs. 8~10).

DISCUSSION

In this study we investigated whether HDAC inhibition promotes functional recovery by polarizing the perilesional environment towards an anti-inflammatory milieu. Our findings indicate

that the non-specific inhibitor scriptaid, reduces the expression of the anti-inflammatory macrophage marker Arg-1 *in vitro*. In contrast, the specific HDAC3 inhibitor RGFP966 increased the expression of Arg-1. Both inhibitors reduced the formation of foamy macrophages. HDAC3 inhibition in a SCI mouse model showed that neither scriptaid nor RGFP966 improved functional recovery or changed the macrophage phenotype *in vivo*.

Our results demonstrate that RGFP966 has no substantial effect on the phenotype of pro-inflammatory macrophages and promotes the alternative activation of macrophages. Similarly, Mulligan et al. [21] showed that HDAC3 restricts many IL-4 targeted genes in macrophages (e.g. Arg-1, Chi3I3 and Clec7a). They demonstrated that HDAC3 deficiency prevents the reduction in IL-4 targeted genes and promotes the switch towards an IL-4 induced alternatively activated macrophage.

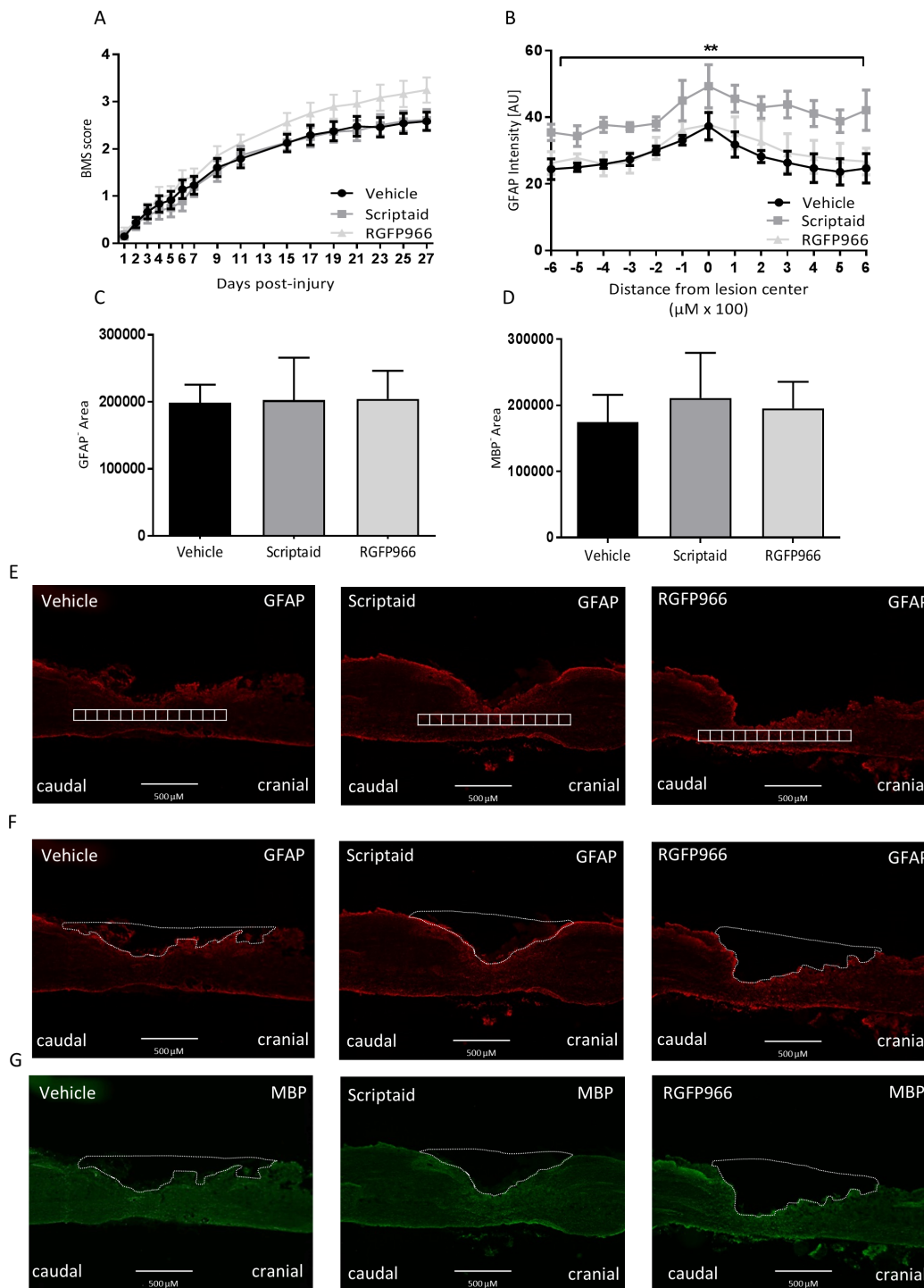


Fig. 8. Scriptaid and RGFP966 have no effect on functional recovery, lesion size or demyelinated area after SCI. BALB/c mice were subjected to a T-cut hemisection SCI. The first 3 days the mice were injected i.p. with scriptaid (3.5 mg/kg), RGFP966 (10 mg/kg) or vehicle. (A) Recovery of hindlimb motor function was determined using the BMS. Treatment with scriptaid or with RGFP966 have no effect on functional recovery after SCI. No changes were observed on lesion size and demyelinated area (C, D, F, G), treatment with scriptaid caused a slight but statistically significant increase in astrogliosis, RGFP966 had no effect on astrogliosis (B, E). Three independent experiments were performed, n=18–23 mice/group (A). Sections were labelled for: GFAP (lesion size, astrogliosis; B, D, E and F) and MBP (demyelinated area; D and G). (E–G) representative images show the method of quantification: GFAP expression was quantified by intensity analysis within rectangular areas of 100 μm×100 μm extending 600 μm cranial to 600 μm caudal from the lesion epicentre. GFAP area and MBP area are delineated to evaluate the lesion size and demyelinated area. Data are represented as means±SEM, n=3 mice/group data from 1 representative experiment are shown. **p<0.01. SCI, spinal cord injury; BMS, Basso Mouse Scale; GFAP, glial fibrillary protein; MBP, myelin basic protein.

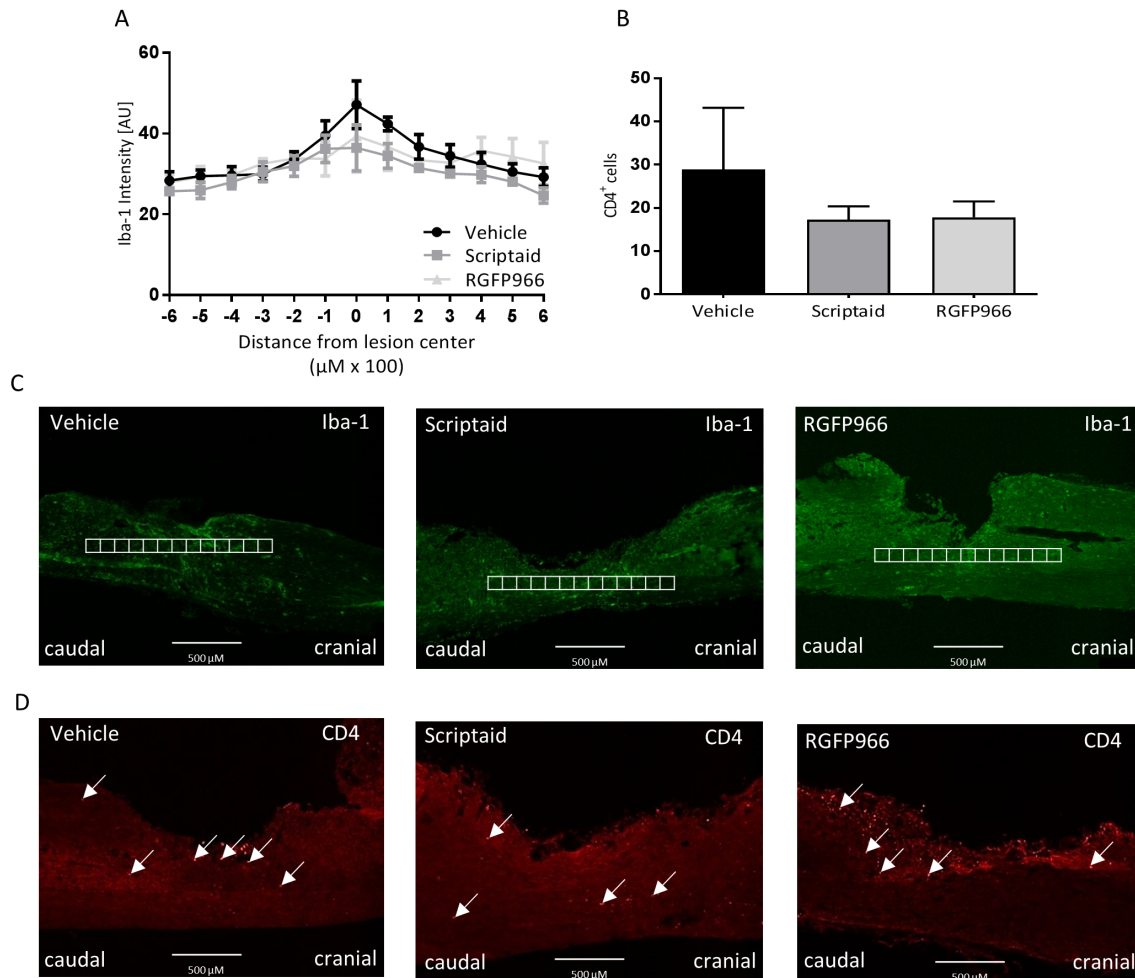


Fig. 9. Scriptaid and RGFP966 have no effect on Iba-1⁺ and CD4⁺ cell immune cell infiltration after SCI. BALB/c mice were subjected to a T-cut hemisection SCI. The first 3 days the mice were injected i.p. with scriptaid (3.5 mg/kg), RGFP966 (10 mg/kg) or vehicle. (A~D) Scriptaid and RGFP966 had no effect on Iba-1⁺ and CD4⁺ cell infiltration. (C, D) Representative images display the method of quantification: Iba-1 expression was quantified by intensity analysis within rectangular areas of 100 μm×100 μm extending 600 μm cranial to 600 μm caudal from the lesion epicentre. The number of CD4⁺ cells was counted and in the representative images the CD4⁺ are indicated with white arrows. Sections were labelled for: Iba-1 (macrophage/microglia infiltration; E) and CD4 (T cell infiltration; F). Data are represented as means±SEM, n=3 mice/group data from 1 representative experiment are shown. **p<0.01. SCI, spinal cord injury; Iba-1, ionized calcium-binding adapter molecule 1 and CD4, cluster of differentiation 4.

Phagocytosis also plays a major role in macrophage polarization. After SCI, macrophages become foamy via phagocytosis of spinal cord debris, thereby converting them to an M1 phenotype [14]. In atherosclerosis, it has been shown that HDAC3 deletion reduces lipid accumulation [30]. Similarly, we wanted to investigate whether HDAC3 inhibition with HDAC inhibitors could decrease the formation of foamy macrophages *in vitro*. We show for the first time, that specific HDAC3 inhibition by RGFP966 significantly reduced the formation of foamy macrophages. This result may contribute to a reduction in the formation of pro-inflammatory M1 macrophages and hence a switch towards a pro-regenerative M2 lesion environment *in vivo*.

Scriptaid, which inhibits HDAC1 and HDAC8 in addition to

HDAC3, displayed differential effects on macrophage phenotype. Unexpectedly, in our hands, scriptaid reduced the protein expression of the M2 marker Arg-1, whereas others have shown that loss of HDAC3 promotes M2 polarization [21]. These contrasting results may be due to the inhibition of HDAC1 besides HDAC3 by scriptaid. HDAC1 has been shown to suppress LPS-induced genes, characteristic for an M1 phenotype, hence inhibition of HDAC1 may lead to M1 macrophage polarization [31]. In addition, previous studies have also shown contradictory results when using HDAC inhibitors depending on the cell type or even within the same cell type. A potential explanation is that HDAC inhibition affects transcription factors that activate diverse sets of genes with contradicting effects as a result [32]. Therefore, future studies

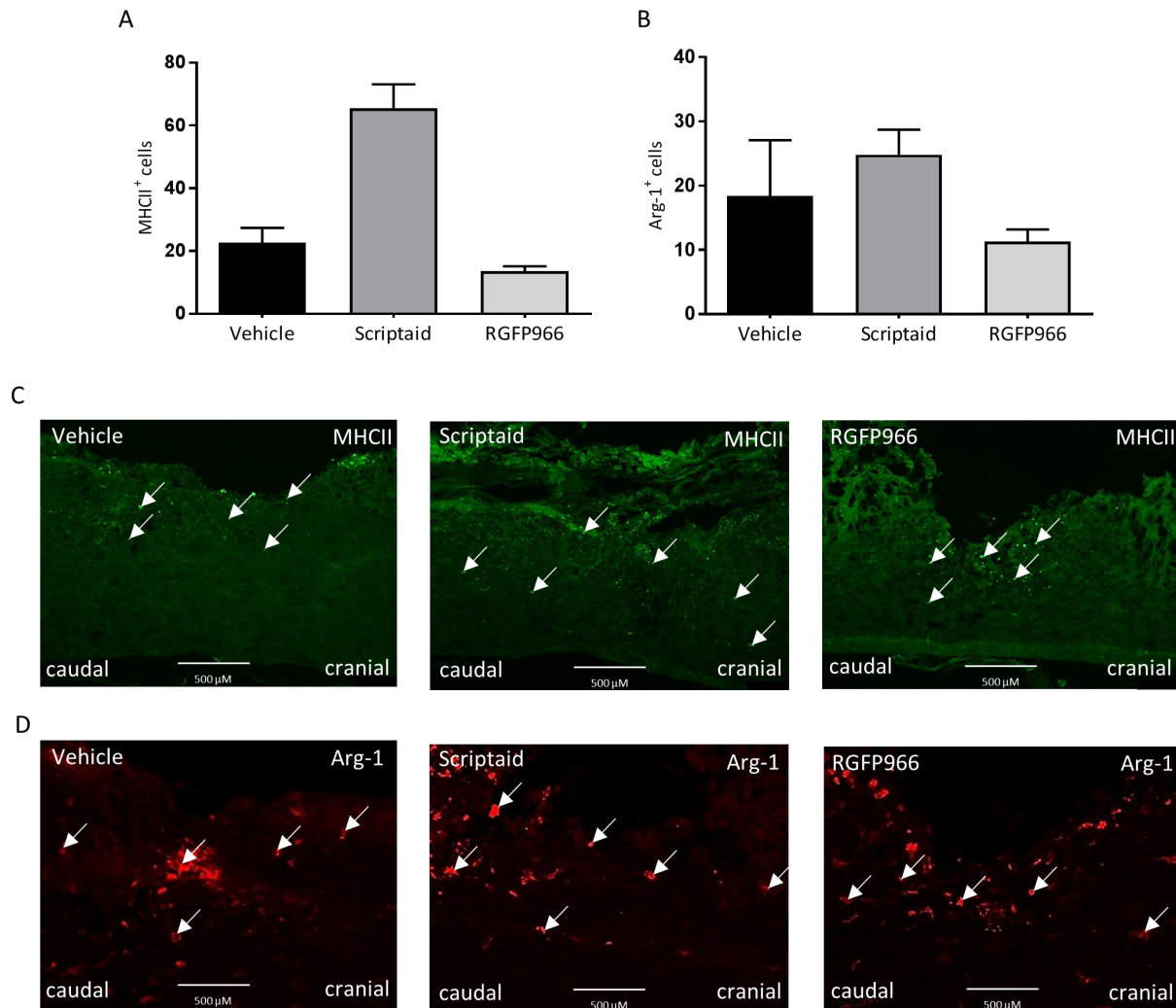


Fig. 10. Scriptaid and RGFP966 have no effect on infiltration of MHCII⁺ and Arg-1⁺ cells after SCI. BALB/c mice were subjected to a T-cut hemisection SCI. The first 3 days the mice were injected i.p. with with scriptaid (3.5 mg/kg), RGFP966 (10 mg/kg) or vehicle. (A~D) Treatment with scriptaid and RGFP966 has no effect infiltration of MHCII⁺ and Arg-1⁺ cells. (C, D) Representative images are shown indicating the MHCII⁺ (C) and Arg-1⁺ (D) with white arrows, these cells were counted at the lesion area. Sections were labelled for: MHCII⁺ cells (classically activated macrophages/microglia; A, C) and Arg-1⁺ cells (alternatively activated macrophages/microglia; B, D). Data are represented as means±SEM, n=3~4 mice/group, data from 1 representative experiment are shown. SCI, spinal cord injury; MHCII, major histocompatibility complex 2 and Arg-1, arginase-1.

should elucidate the signalling pathways modulated by HDACs to gain better understanding of the underlying mechanisms when using HDAC inhibitors as a treatment for CNS disorders.

Both inhibitors were administered individually in the T-cut hemisection mouse model and we monitored the functional recovery using the BMS. Surprisingly, neither scriptaid nor RGFP966 affected functional recovery. Consistently, the histological analyses indicated no differences between the treatment groups and the control groups.

In a parallel study, it was shown that RGFP966 significantly improved functional recovery after a *contusion* SCI [33]. The different outcomes may be due to the use of different mouse models.

A typical characteristic of a contusion injury, used by Kuboyama et al. [33], is the presence of spared fibers. In our T-cut hemisection model of SCI, we completely transect the dorsomedial and ventral corticospinal tract ruling out spared fibers, which is in contrast to a contusion and regular hemisection injury [34]. Interestingly, Kuboyama et al. analyzed the effects of RGFP966 on the immune response in a transection model of SCI similar to our model but did not show functional BMS data [33]. In the contusion injury model, functional recovery may be accelerated and biased by spared fibers and by collateral sprouting, whereas in the T-cut hemisection model, the precisely cut motor tracts need to truly regenerate [34, 35]. HDAC3 inhibition may have stimulated

recovery of spared fibers in the contusion injury model used by Kuboyama et al., considering that HDAC inhibition has been shown to have neuroprotective and axon growth promoting effects [36, 37]. Future studies will be required to investigate whether the effects of HDAC3 inhibition in the contusion injury model are mediated via the preservation of spared fibers.

In conclusion, HDAC3 inhibition by RGFP966 promotes the alternative activation of macrophages and reduces the formation of foamy pro-inflammatory macrophages *in vitro* but does not affect functional recovery in the T-cut hemisection model of SCI.

ACKNOWLEDGEMENTS

The authors thank Dr. Leen Timmermans (Hasselt University) for excellent technical support. This study was supported in part by grants from 'Fonds voor Wetenschappelijk Onderzoek – Vlaanderen' (FWO) to SH (GOA1413, G0A5813FWO, G0667715N). This funding did not lead to any conflict of interests. All authors declare that there is no conflict of interest. Data from this study was presented as a poster by Selien Sanchez at the 2017 BIS meeting in Leuven, Belgium. Part of the data from this study was generated by Paulien Baeten during her master thesis internship.

DATA AVAILABILITY STATEMENT

The data used to support the findings of this study are available from the corresponding author upon request.

REFERENCES

- Bowes AL, Yip PK (2014) Modulating inflammatory cell responses to spinal cord injury: all in good time. *J Neurotrauma* 31:1753-1766.
- Gaudet AD, Popovich PG (2014) Extracellular matrix regulation of inflammation in the healthy and injured spinal cord. *Exp Neurol* 258:24-34.
- Shechter R, Schwartz M (2013) CNS sterile injury: just another wound healing? *Trends Mol Med* 19:135-143.
- Dooley D, Lemmens E, Vanganswinkel T, Le Blon D, Hoor-naert C, Ponsaerts P, Hendrix S (2016) Cell-based delivery of interleukin-13 directs alternative activation of macrophages resulting in improved functional outcome after spinal cord injury. *Stem Cell Reports* 7:1099-1115.
- Nelissen S, Vanganswinkel T, Geurts N, Geboes L, Lemmens E, Vidal PM, Lemmens S, Willems L, Boato F, Dooley D, Pehl D, Pejler G, Maurer M, Metz M, Hendrix S (2014) Mast cells protect from post-traumatic spinal cord damage in mice by degrading inflammation-associated cytokines via mouse mast cell protease 4. *Neurobiol Dis* 62:260-272.
- Vanganswinkel T, Geurts N, Quanten K, Nelissen S, Lemmens S, Geboes L, Dooley D, Vidal PM, Pejler G, Hendrix S (2016) Mast cells promote scar remodeling and functional recovery after spinal cord injury via mouse mast cell protease 6. *FASEB J* 30:2040-2057.
- Lemmens S, Kusters L, Bronckaers A, Geurts N, Hendrix S (2017) The β 2-adrenoceptor agonist terbutaline stimulates angiogenesis via Akt and ERK signaling. *J Cell Physiol* 232:298-308.
- David S, Greenhalgh AD, Kroner A (2015) Macrophage and microglial plasticity in the injured spinal cord. *Neuroscience* 307:311-318.
- David S, Kroner A (2011) Repertoire of microglial and macrophage responses after spinal cord injury. *Nat Rev Neurosci* 12:388-399.
- Kigerl KA, Gensel JC, Ankeny DP, Alexander JK, Donnelly DJ, Popovich PG (2009) Identification of two distinct macrophage subsets with divergent effects causing either neurotoxicity or regeneration in the injured mouse spinal cord. *J Neurosci* 29:13435-13444.
- Busch SA, Horn KP, Silver DJ, Silver J (2009) Overcoming macrophage-mediated axonal dieback following CNS injury. *J Neurosci* 29:9967-9976.
- Horn KP, Busch SA, Hawthorne AL, van Rooijen N, Silver J (2008) Another barrier to regeneration in the CNS: activated macrophages induce extensive retraction of dystrophic axons through direct physical interactions. *J Neurosci* 28:9330-9341.
- Busch SA, Hamilton JA, Horn KP, Cuascut FX, Cutrone R, Lehman N, Deans RJ, Ting AE, Mays RW, Silver J (2011) Multipotent adult progenitor cells prevent macrophage-mediated axonal dieback and promote regrowth after spinal cord injury. *J Neurosci* 31:944-953.
- Wang X, Cao K, Sun X, Chen Y, Duan Z, Sun L, Guo L, Bai P, Sun D, Fan J, He X, Young W, Ren Y (2015) Macrophages in spinal cord injury: phenotypic and functional change from exposure to myelin debris. *Glia* 63:635-651.
- Ren Y, Young W (2013) Managing inflammation after spinal cord injury through manipulation of macrophage function. *Neural Plast* 2013:945034.
- Kazantsev AG, Thompson LM (2008) Therapeutic application of histone deacetylase inhibitors for central nervous system disorders. *Nat Rev Drug Discov* 7:854-868.
- Abdanipour A, Schluesener HJ, Tiraihi T (2012) Effects of valproic acid, a histone deacetylase inhibitor, on improve-

- ment of locomotor function in rat spinal cord injury based on epigenetic science. *Iran Biomed J* 16:90-100.
18. Wu C, Li A, Leng Y, Li Y, Kang J (2012) Histone deacetylase inhibition by sodium valproate regulates polarization of macrophage subsets. *DNA Cell Biol* 31:592-599.
 19. Wang G, Shi Y, Jiang X, Leak RK, Hu X, Wu Y, Pu H, Li WW, Tang B, Wang Y, Gao Y, Zheng P, Bennett MV, Chen J (2015) HDAC inhibition prevents white matter injury by modulating microglia/macrophage polarization through the GSK3 β /PTEN/Akt axis. *Proc Natl Acad Sci U S A* 112:2853-2858.
 20. Huber K, Doyon G, Plaks J, Fyne E, Mellors JW, Sluis-Cremer N (2011) Inhibitors of histone deacetylases: correlation between isoform specificity and reactivation of HIV type 1 (HIV-1) from latently infected cells. *J Biol Chem* 286:22211-22218.
 21. Mullican SE, Gaddis CA, Alenghat T, Nair MG, Giacomini PR, Everett LJ, Feng D, Steger DJ, Schug J, Artis D, Lazar MA (2011) Histone deacetylase 3 is an epigenomic brake in macrophage alternative activation. *Genes Dev* 25:2480-2488.
 22. Rios FJ, Touyz RM, Montezano AC (2017) Isolation and differentiation of human macrophages. *Methods Mol Biol* 1527:311-320.
 23. Malvaez M, McQuown SC, Rogge GA, Astarabadi M, Jacques V, Carreiro S, Rusche JR, Wood MA (2013) HDAC3-selective inhibitor enhances extinction of cocaine-seeking behavior in a persistent manner. *Proc Natl Acad Sci U S A* 110:2647-2652.
 24. Boato F, Hendrix S, Huelsenbeck SC, Hofmann E, Grosse G, Djalali S, Klimaschewski L, Auer M, Just I, Ahnert-Hilger G, Höltje M (2010) C3 peptide enhances recovery from spinal cord injury by improved regenerative growth of descending fiber tracts. *J Cell Sci* 123:1652-1662.
 25. Wang G, Jiang X, Pu H, Zhang W, An C, Hu X, Liou AK, Leak RK, Gao Y, Chen J (2013) Scriptaid, a novel histone deacetylase inhibitor, protects against traumatic brain injury via modulation of PTEN and AKT pathway: scriptaid protects against TBI via AKT. *Neurotherapeutics* 10:124-142.
 26. Basso DM, Fisher LC, Anderson AJ, Jakeman LB, McTigue DM, Popovich PG (2006) Basso mouse scale for locomotion detects differences in recovery after spinal cord injury in five common mouse strains. *J Neurotrauma* 23:635-659.
 27. McWhorter FY, Wang T, Nguyen P, Chung T, Liu WF (2013) Modulation of macrophage phenotype by cell shape. *Proc Natl Acad Sci U S A* 110:17253-17258.
 28. Gensel JC, Zhang B (2015) Macrophage activation and its role in repair and pathology after spinal cord injury. *Brain Res* 1619:1-11.
 29. Pesce JT, Ramalingam TR, Mentink-Kane MM, Wilson MS, El Kasmi KC, Smith AM, Thompson RW, Cheever AW, Murray PJ, Wynn TA (2009) Arginase-1-expressing macrophages suppress Th2 cytokine-driven inflammation and fibrosis. *PLoS Pathog* 5:e1000371.
 30. Hoeksema MA, Gijbels MJ, Van den Bossche J, van der Velden S, Sijm A, Neele AE, Seijkens T, Stöger JL, Meiler S, Boshuizen MC, Dallinga-Thie GM, Levels JH, Boon L, Mullican SE, Spann NJ, Cleutjens JP, Glass CK, Lazar MA, de Vries CJ, Biessen EA, Daemen MJ, Lutgens E, de Winther MP (2014) Targeting macrophage Histone deacetylase 3 stabilizes atherosclerotic lesions. *EMBO Mol Med* 6:1124-1132.
 31. Halili MA, Andrews MR, Labzin LI, Schroder K, Matthias G, Cao C, Lovelace E, Reid RC, Le GT, Hume DA, Irvine KM, Matthias P, Fairlie DP, Sweet MJ (2010) Differential effects of selective HDAC inhibitors on macrophage inflammatory responses to the Toll-like receptor 4 agonist LPS. *J Leukoc Biol* 87:1103-1114.
 32. Dietz KC, Casaccia P (2010) HDAC inhibitors and neurodegeneration: at the edge between protection and damage. *Pharmacol Res* 62:11-17.
 33. Kuboyama T, Wahane S, Huang Y, Zhou X, Wong JK, Koemeter-Cox A, Martini M, Friedel RH, Zou H (2017) HDAC3 inhibition ameliorates spinal cord injury by immunomodulation. *Sci Rep* 7:8641.
 34. Steward O, Zheng B, Tessier-Lavigne M (2003) False resurrections: distinguishing regenerated from spared axons in the injured central nervous system. *J Comp Neurol* 459:1-8.
 35. Tuszynski MH, Steward O (2012) Concepts and methods for the study of axonal regeneration in the CNS. *Neuron* 74:777-791.
 36. Gaub P, Tedeschi A, Puttagunta R, Nguyen T, Schmandke A, Di Giovanni S (2010) HDAC inhibition promotes neuronal outgrowth and counteracts growth cone collapse through CBP/p300 and P/CAF-dependent p53 acetylation. *Cell Death Differ* 17:1392-1408.
 37. Wu X, Chen PS, Dallas S, Wilson B, Block ML, Wang CC, Kinyamu H, Lu N, Gao X, Leng Y, Chuang DM, Zhang W, Lu RB, Hong JS (2008) Histone deacetylase inhibitors up-regulate astrocyte GDNF and BDNF gene transcription and protect dopaminergic neurons. *Int J Neuropsychopharmacol* 11:1123-1134.